Chemical profiles of birch and alder bark by ambient mass spectrometry

Räsänen, Riikka-Marjaana

2019-11

Räsänen , R-M , Hieta , J-P , Immanen , J , Nieminen , K , Haavikko , R , Yli-Kauhaluoma , J & Kauppila , T J 2019 , ' Chemical profiles of birch and alder bark by ambient mass spectrometry ' , Analytical and Bioanalytical Chemistry , vol. 411 , no. 28 , pp. 7573-7583 . https://doi.org/10.1007/s0

http://hdl.handle.net/10138/308039
https://doi.org/10.1007/s00216-019-02171-9

Analytical and Bioanalytical Chemistry (2019) 411:7573–7583
https://doi.org/10.1007/s00216-019-02171-9

RESEARCH PAPER

Chemical profiles of birch and alder bark by ambient mass spectrometry

Riikka-Marjaana Räsänen[1] · Juha-Pekka Hieta[1] · Juha Immanen[2] · Kaisa Nieminen[2] · Raisa Haavikko[1] · Jari Yli-Kauhaluoma[1] · Tiina J. Kauppila[3]

Received: 10 July 2019 / Revised: 11 September 2019 / Accepted: 24 September 2019 / Published online: 23 October 2019

Abstract

Desorption atmospheric pressure photoionization (DAPPI) is an ambient mass spectrometry (MS) technique that allows the analysis of both polar and nonpolar compounds directly from the surfaces of various sample types. Here, DAPPI was used to study the chemical profiles in different parts of birch and alder tree barks. Four distinct fractions of *Betula pendula* (silver birch) bark were collected from three different developmental stages of the stem, after which the chemical profiles of the different tissue types were measured. Of special interest were triterpenoids, a class of important defensive substances, which are found in the bark of the silver birch. Additionally, the chemical profiles of lenticels and the surrounding surfaces in the phellem of *B. pendula* (silver birch), *Alnus glutinosa* (black alder), and *Alnus incana* (gray alder) were screened with DAPPI. Another ambient MS technique, laser ablation atmospheric pressure photoionization (LAAPPI), was further used for the mass spectrometry imaging of lenticels on the *B. pendula* phellem. All the studied birch bark fractions showed individual chemical profiles in DAPPI. The mass spectra from the young apical stem and the transition zone resembled each other more than the mature stem. Instead, the phellem was found to contain a high amount of triterpenoids in all the developmental stages of the stem. The most intense peaks in the DAPPI mass spectra of the birch bark fractions were those of betulin and lupeol. Betulinic and betulonic acid peaks were intense as well, and these compounds were detected especially in the lenticels of the tree samples.

Keywords Triterpenoid · Bark · Desorption atmospheric pressure photoionization · Laser ablation atmospheric pressure photoionization · Ambient mass spectrometry · Mass spectrometry imaging

Introduction

It has been reported that over 50% of currently sold pharmaceuticals originate from natural products or naturally occurring compounds or their derivatives synthesized in the laboratory [1]. One natural compound that has proved to have interesting bioactivities is the triterpenoid betulin, and especially its natural derivatives like betulinic acid [2–4]. These compounds have been used as scaffolds in various drug development projects that aim at treatments of, e.g., bacterial inflammations [5] and cancer [6]. The structures of betulin and some other triterpenoids are presented in Fig. 1. In nature, betulin and its derivatives exist abundantly in the bark of *Betula* spp., especially in *Betula pendula* (silver birch) [4], but they are also found in the bark of many *Alnus* spp. [7, 8] which belong to the same family of Betulaceae. Bark is the outermost layer of the tree, and it consists of fractions with distinct tissue types. A schematic picture of the *B. pendula* bark structure containing four fractions (phellem, phelloderm/phellogen, old phloem, and developing phloem) is presented in

Electronic supplementary material The online version of this article (https://doi.org/10.1007/s00216-019-02171-9) contains supplementary material, which is available to authorized users.

✉ Riikka-Marjaana Räsänen
rmrasane@gmail.com

✉ Tiina J. Kauppila
tiina.kauppila@helsinki.fi

[1] Drug Research Program, Division of Pharmaceutical Chemistry and Technology, Faculty of Pharmacy, P.O. Box 56, FI-00014 University of Helsinki, Helsinki, Finland

[2] Natural Resources Institute Finland (Luke), Production Systems, Plant Genetics, Viikinkaari 1, FI-00790 Helsinki, Finland

[3] Finnish Institute for Verification of the Chemical Weapons Convention (VERIFIN), Department of Chemistry, P.O. Box 55, FI-00014 University of Helsinki, Helsinki, Finland

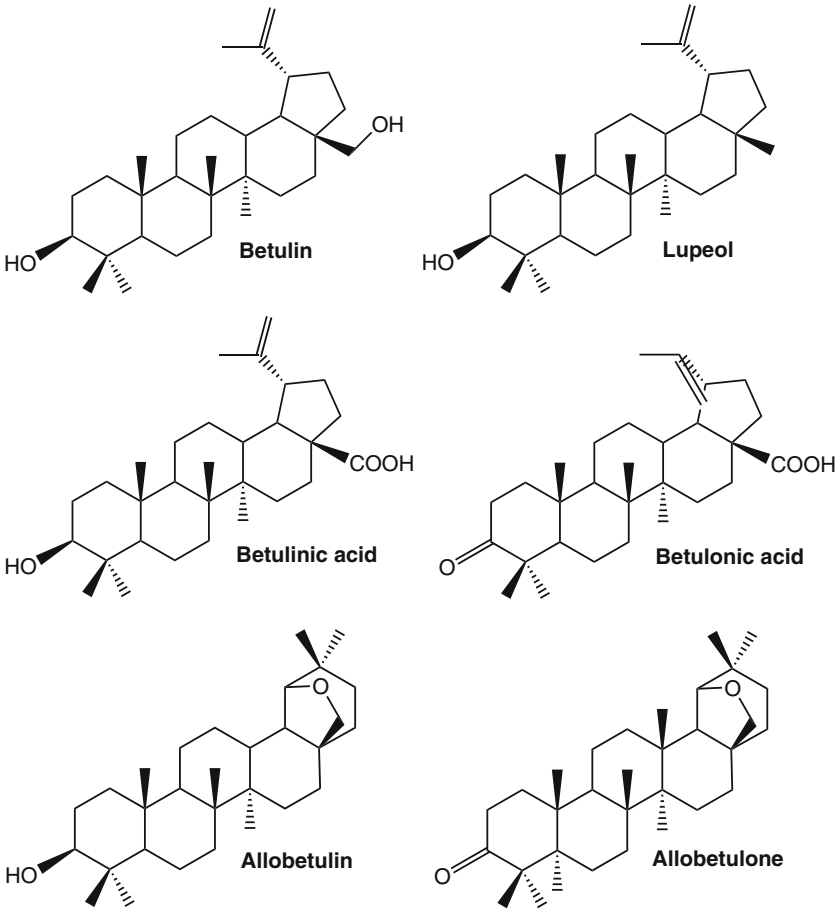

Fig. 1 Structures of triterpenoids used in this study

Fig. 2. The color and the roughness of the bark surface are diverse for different tree species, and the appearance of the bark is also affected by lenticels, channels that enable the gas exchange from the surrounding atmosphere to the inner structures of the tree. Betulin and its derivatives are located mainly in the phellem, which is the outermost fraction of the bark [9].

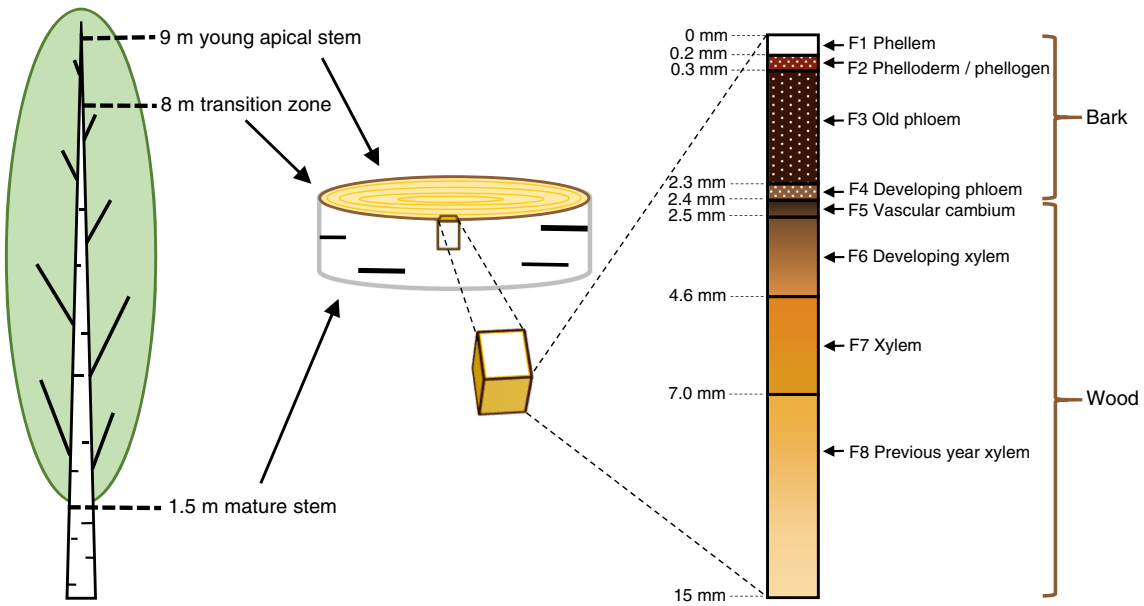

Fig. 2 A schematic picture of the sampled fractions across vascular cambium of the *B. pendula* stem, tree samples, and the different fractions in the stem

Plants produce a vast and diverse array of metabolites and recent years have seen a surge of interest in their biotechnological potential. Complex plant samples containing plant metabolites are traditionally analyzed by multistep analytical techniques, such as gas chromatography (GC) or liquid chromatography (LC) separation coupled with mass spectrometry (MS) detection [10]. These methods require careful sample pretreatment with often several time-consuming steps, which increase the total analysis time remarkably. Additionally, large sample pieces are required for the pretreatment, and therefore small changes in the spatial distribution of the metabolites in the sample will be lost. For solid samples like plant leafs [11], fast surface sampling and analysis by ambient MS is also feasible. In ambient MS, the compounds are sampled directly from the surface in atmospheric pressure conditions and detected by MS [12]. Ambient MS techniques can be used for the rapid screening of compounds from the surfaces of, e.g., plants, tablets, or dried blood spots without prior sample preparation [13]. In addition, ambient MS makes possible the determination of the spatial distribution of different analytes in the sample, as in, e.g., mass spectrometry imaging of animal tissues [14], or plant metabolites [15].

Desorption atmospheric pressure photoionization-mass spectrometry (DAPPI-MS) is an ambient MS technique, which can be used for the efficient detection of both polar and nonpolar compounds [16]. In DAPPI, the sampling surface is exposed to a hot solvent spray, which causes thermal desorption of the compounds from the surface (Fig. 3). The vaporized compounds are ionized through a series of reactions initiated by photons emitted from a vacuum ultraviolet (VUV) lamp, and the formed ions are directed to the MS for analysis. The ionization process in DAPPI has been reported to be similar to that in atmospheric pressure photoionization (APPI) [17]. The hot solvent spray acts as a dopant, which participates in the ionization process and enhances the ionization efficiency. The selection of the right type of dopant for the experiment is important. Earlier DAPPI studies have shown that acetone and toluene are efficient DAPPI dopants [13, 16, 17]. When toluene is used as a dopant, the formed analyte ions will be mainly molecular ions or protonated molecules, and when acetone is used, protonated molecules are formed. In plant analysis, DAPPI has been used to analyze cannabinoids from *Cannabis sativa* blooms [18], cathine from *Catha edulis* leaves [19], neonicotinoids from rose leafs [20], metabolites from *Peucedanum palustre* leafs [11], and -tocopherol (vitamin E) from almond tree seeds [13]. Like APPI, also DAPPI is a very sensitive ionization technique for low polarity compounds [13, 16, 17, 21], which is beneficial in the plant analysis, since many plant metabolites have low polarities.

Another ambient MS technique based on photoionization is laser ablation atmospheric pressure photoionization (LAAPPI) [22]. In LAAPPI, the analytes are ablated from the sample surface with infrared (IR) laser and ionized through photoionization reactions. Thanks to the laser ablation, LAAPPI achieves an excellent spatial resolution of less than 50 m [23], and therefore it is feasible for mass spectrometry

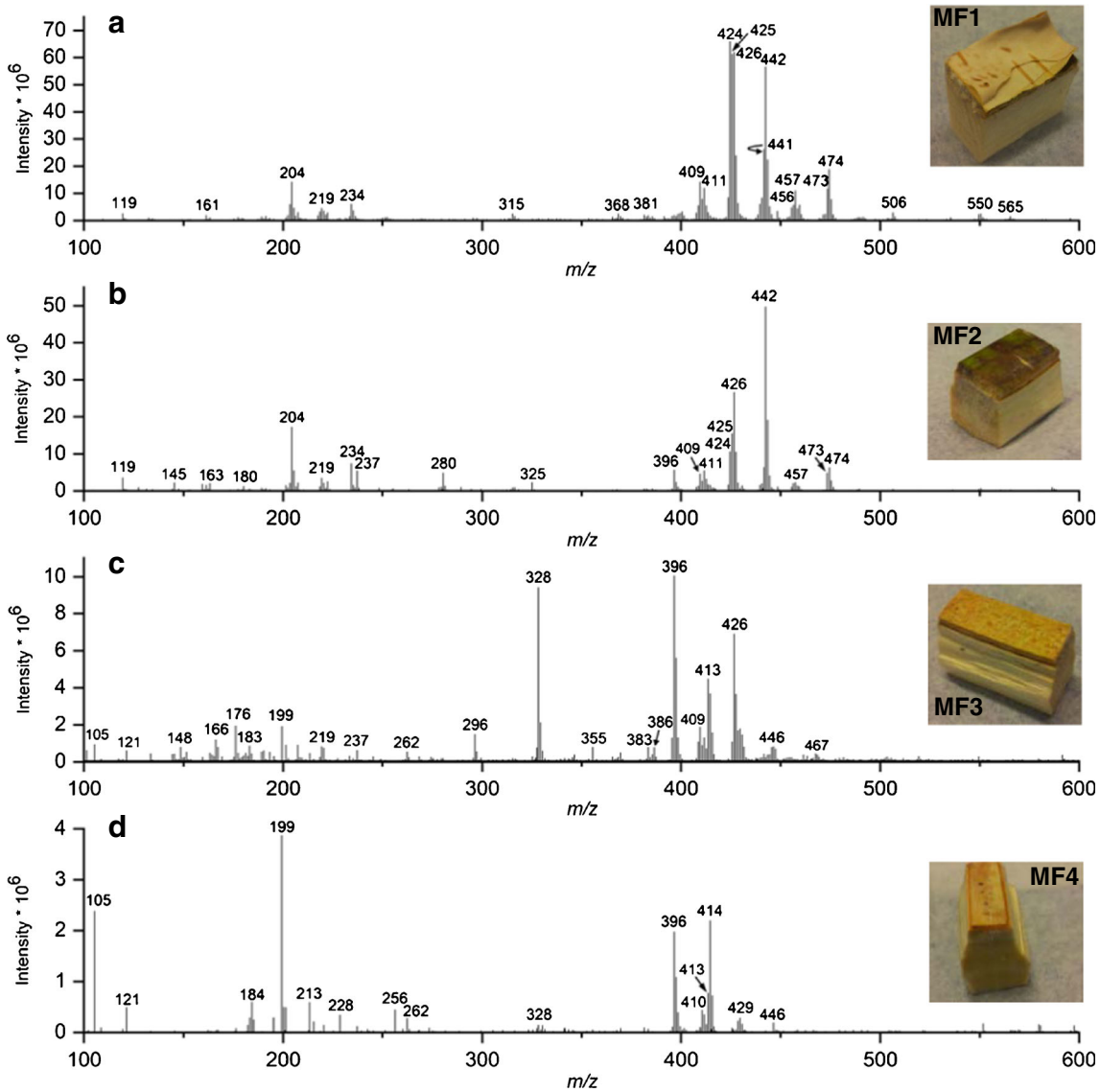

Fig. 5 The DAPPI mass spectra of *B. pendula* MF1–MF4 in positive ion mode using toluene as the dopant: **a** MF1, **b** MF2, **c** MF3, and **d** MF4. Photos of the bark samples are also presented

measurements and GC-MS measurements made from the bark samples for the identification of betulin, lupeol, betulinic acid, betulonic acid, allobetulin, and allobetulone ions. For the ions at *m*/z 424 and 425, the identification was supported by the MS and MS^2 data of the samples and the standards (Table 2 and ESM Table S2). Tentative origins for some of the high-intensity ions detected from the samples are also suggested in the text as they are supported by literature and/or the experimental data.

The ions at *m*/*z* 442 and 426 were identified as $M^{+\bullet}$ of betulin and lupeol, respectively. The ion at *m*/*z* 443 was thought to be a combination of allobetulin $[M + H]^+$ and betulin $M^{+\bullet}$ C^{13} isotopes, and the ion at *m*/*z* 427 was presumed to be mainly the lupeol C^{13} isotope, since lupeol did not protonate in direct infusion APPI studies of triterpenoids (Table 1). The ion at *m*/*z* 441 was identified as the $[M + H]^+$ of allobetulone. Betulinic acid was detected as $M^{+\bullet}$ at *m*/z 456 and betulonic acid as both $[M + H]^+$ and $M^{+\bullet}$ at *m*/*z* 455 and *m*/z 454, respectively. The ion at *m*/*z* 204 (Fig. 5a, b) could be a fragment of lupeol, since it was the main product ion of lupeol $M^{+\bullet}$ in APPI MS^2 experiments (ESM Table S1). The ion at *m*/*z* 424 was assumed to be the $[M\text{-}H_2O]^+$ fragment of betulin (ESM Table S1). It was ruled out to originate from allobetulin, since the DAPPI-MS^2 experiments of the *m*/*z* 442 ion from the birch bark did not show the allobetulin fragment ion at *m*/*z* 371 (ESM Table S1), and as a whole, the MS^2 spectrum of the ion at *m*/z 442 corresponded to betulin $M^{+\bullet}$ MS^2 spectrum. Therefore, it was concluded that the bark samples did not show $M^{+\bullet}$ of allobetulin. The ion at *m*/*z* 425 was assumed to be the $[M + H\text{-}H_2O]^+$ of betulin [32–34] or allobetulin, as it was observed in the APPI experiments with acetone dopant for both compounds (Table 1 and ESM Table S2). The ions at

m/z 409 and 411 were typical product ions for many of the triterpenoids (ESM Table S1). An intense group of ions related to the triterpenoids can be observed in Fig. 5a, b in the mass range of approx. 470–475. These ions are suggested to be the oxidation products of the triterpenoid acids.

The ions at *m*/z 105, 121, 176, 199, 296, 328, 396, 413, 414, and 415, presented in Fig. 5, which contribute to the separation of fractions F2–F4 of transition zone and young apical stem, and the samples MF3 and MF4 from all the F1 samples in the PCA (Fig. 4), were not identified, but they are suggested to be other plant metabolites present in the bark. For example, according to literature, the phytosterol -sitosterol (molecular weight 414 Da) is present in the birch bark [37, 38], and was detected in GC-MS experiments conducted from samples from the same trees as in this study (unpublished results). -Sitosterol shows $M^{+\bullet}$ at *m*/*z* 414, and a $[M\text{-}H_2O]^+$ fragment at *m*/z 396 in electron ionization-mass spectrum [39]. Therefore, the ions at *m*/*z* 396 and 414 (Fig. 5d) are suggested to originate from -sitosterol. Additionally, the natural arylbutanoid glycoside rhododendrin with molecular weight of 328 is present in the inner bark of *B. pendula* [40, 41], and therefore the ion at *m*/*z* 328 in Fig. 5c, d could be due to the $M^{+\bullet}$ of rhododendrin. In negative ion electrospray ionization (ESI), rhododendrin has been detected as $[M\text{-}H]^-$ at *m*/*z* 327 [41], and in positive ion ESI as $[M + 23]^+$ at *m*/*z* 351 [40].

It can be concluded that the triterpenoids dominate the chemical profile of the *B. pendula* bark fractions F1 and MF2, which contain a high amount of triterpenoids, including, e.g., betulin, lupeol, betulinic acid, and betulonic acid, even though the concentrations of the triterpenoids decrease in the order of mature stem > transition zone > young apical stem [9]. Compared to F1, the other fractions in all the developmental stages lack triterpenoids. Instead, they are rich with other plant metabolites, such as -sitosterol and rhododendrin.

Analysis of lenticels of *B. pendula*, *A. glutinosa*, and *A. incana* by DAPPI-MS

DAPPI-MS was used to study the lenticels and the surrounding surface from the F1 of the bark of *B. pendula*, *A. glutinosa*, and *A. incana*. Figure 6 presents the mass spectra from YF1 of *B. pendula* (Fig. 6a, b) and MF1 of *A. glutinosa* (Fig. 6c, d) samples, and shows photographs of the samples. Both bark samples contained clear light-colored lenticels surrounded by darker surface, which in the young apical stem surface of *B. pendula* is brown and in *A. glutinosa* dark gray. For both tree species, it was found that the lenticels and the surrounding tissue contain distinct chemical compositions (Fig. 6).

For *B. pendula*, the F1 surface showed a high amount of triterpenoids (Fig. 6a), as discussed above. The betulin $M^{+\bullet}$, its propable fragment $[M\text{-}H_2O]^+$, and allobetulone $[M + H]^+$ at *m*/*z* 442, 424, and 441, respectively, were observed with high abundances in the tissue surrounding the lenticels. In the lenticels, betulinic and betulonic acids, detected as $[M + H]^+$ at *m*/*z* 456 and 455, respectively, were the main triterpenoids (Fig. 6b) at higher abundance than in the surrounding tissue (Fig. 6a). The ion at *m*/z 439 was assumed to be a combination of fragments of betulonic and betulinic acids, respectively (ESM Table S1). Instead, the intensities of betulin and lupeol $M^{+\bullet}$ ions at *m*/*z* 442 and 426, respectively, in the lenticels were negligible compared to the surrounding surface.

For *A. glutinosa*, the surface of the phellem (excluding the lenticels) contained only a small amount of triterpenoids (Fig. 6c) and for example the betulin $M^{+\bullet}$ abundance was approx. 5% of the intensity of what was measured from the YF1 samples of *B. pendula*. Instead, the lenticels of *A. glutinosa* showed high abundancies for triterpenoids in the *m*/z range of approx. 400–480 in Fig. 6d. The highest triterpenoid intensity was measured for lupeol $M^{+\bullet}$ at *m*/*z* 426. The intensities of betulonic acid $[M + H]^+$ and betulinic acid $M^{+\bullet}$, at *m*/*z* 455 and 456, respectively, were approximately five times higher in the lenticels than in the surface surrounding the lenticels. The ions at *m*/*z* 409 and 410 are possibly the fragments of betulonic acid $[M + H]^+$ and $M^{+\bullet}$ ions (ESM Table S1), and the ion at *m*/*z* 439 the fragment of betulonic and betulinic acids, as described previously. The intense ion at *m*/*z* 248 may be a fragment of both betulonic and betulinic acid $M^{+\bullet}$ (ESM Table S1), and it is observed in the mass spectrum of the lenticel measurements from both *B. pendula* and *A. glutinosa* (Fig. 6b, d). Again, the $[M + H\text{-}H_2O]^+$ ion at *m*/*z* 425 is most likely to originate from betulin [34] or allobetulin $[M + H]^+$ (Table 1 and ESM Table S2). The allobetulone $[M + H]^+$ ion at *m*/*z* 441 was also detected. The higher abundancies of betulinic and betulonic acids in the lenticels compared to the surrounding bark surface may be due to the efficient oxidizing reaction of the betulin taken place at the lenticels, which act as gas exchange channels between the atmosphere and the inner parts of the tree.

The color of the lenticels in the *A. incana* F1 surface was much lighter than in the lenticels on *A. glutinosa*, almost indistinguishable from the surrounding bark area. The surrounding surface contained clear light gray and dark gray areas (see ESM, Fig. S2). The light and dark areas, as well as the lenticels, were analyzed separately by DAPPI-MS, and the mass spectra are presented in the ESM in Fig. S3. Triterpenoids were detected from the lenticels (ESM Fig. S3a), but the intensities were much lower than in the *A. glutinosa* F1 samples. The main triterpenoid detected was the lupeol $M^{+\bullet}$ at *m*/*z* 426. Betulonic acid $[M + H]^+$ and betulinic acid $M^{+\bullet}$ were detected at *m*/*z* 455 and 456, respectively, as well as the ion at *m*/*z* 439, most likely originating from both betulonic and betulinic acids. None of the triterpenoids was detected from the surrounding tissue. However, the mass spectra of the light (ESM Fig. S3b) and dark gray (ESM Fig. S3c) areas were very distinct from each other. In the light area, the two most

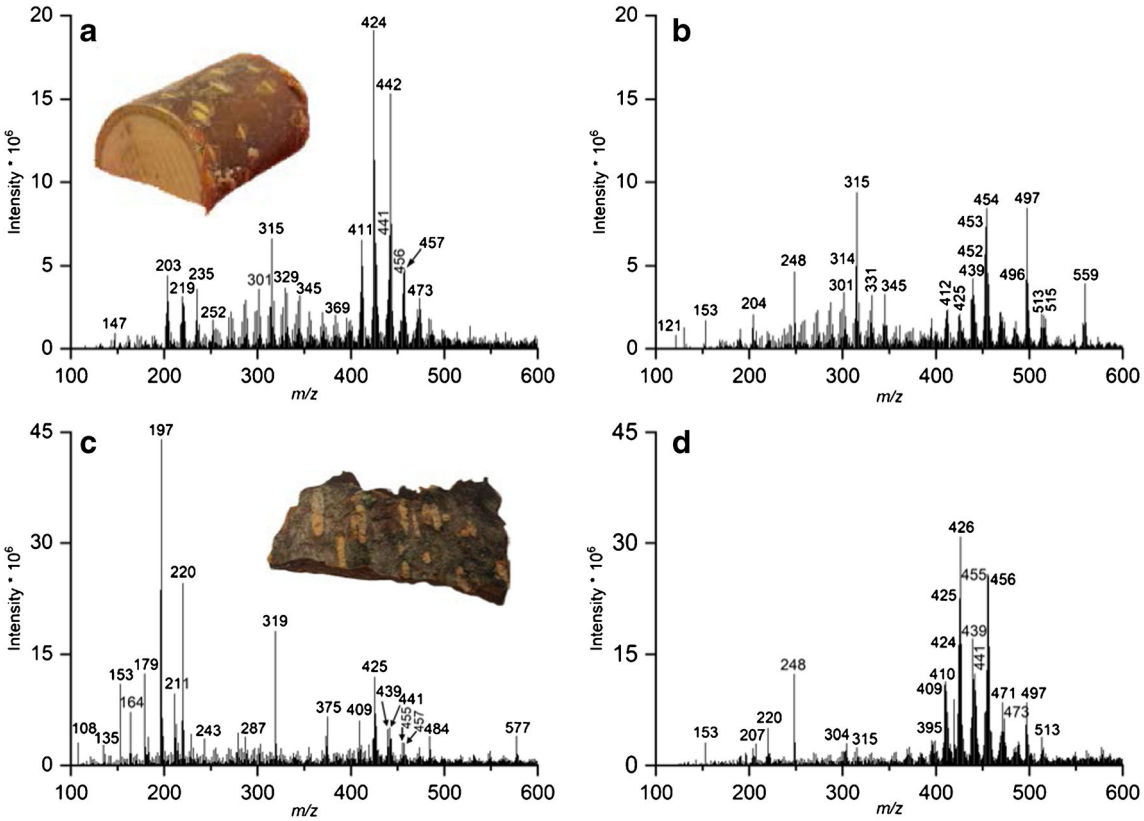

Fig. 6 DAPPI mass spectra of *B. pendula* YF1 and *A. glutinosa* MF1 analysis of lenticels and the surrounding surface and example photographs of the samples. The measurements were done in positive ion mode using toluene as the dopant. **a** *B. pendula* surrounding surface analysis, **b** *B. pendula* lenticel analysis, **c** *A. glutinosa* surrounding surface analysis, and **d** *A. glutinosa* lenticel analysis

abundant ions were observed at *m/z* 196 and 220, but in the dark gray area two intense ions appeared at *m/z* 345 and 467. However, these ions remain unidentified.

LAAPPI-MSI of *B. pendula* lenticels

DAPPI utilizes a wide and continuous solvent plume for sampling, and thus the technique's ability to locate compounds could be questioned. LAAPPI, instead, enabled spatially precise sampling of the F1 surface. Here, LAAPPI-MSI was used to study the distributions of all the previously detected triterpenoids at *B. pendula* F1 lenticel regions. The distribution of betulinic acid was of particular interest, as DAPPI-MS showed betulinic acid to be more abundant at the F1 lenticel regions than the other areas on the F1 surface.

Acetone was chosen as the dopant for the LAAPPI-MSI measurements, because it drives the ionization process toward formation of protonated molecules, and this simplifies the surface screening analysis. Moreover, DAPPI-MS and APPI-MS experiments with acetone showed that most triterpenoids can be detected with at least one characteristic mass peak.

LAAPPI-MS detected all the same triterpenoids as DAPPI-MS (Table 1). Furthermore, the created heat map images show clear betulinic acid distribution patterns around the F1 lenticel regions as presented in Fig. 7. Betulinic acid was found to be much more abundant at the lenticel regions of F1 (deep red color) compared to the surrounding tissue, as was observed with DAPPI-MS as well. All other triterpenoids were more

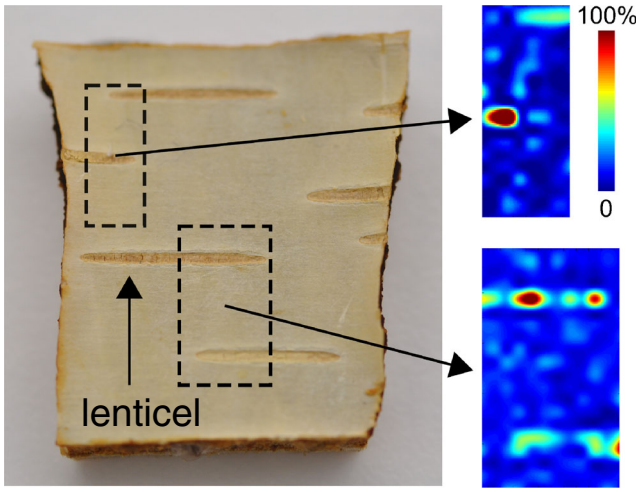

Fig. 7 The distribution of betulinic acid in MF1 fraction of *B. pendula* measured by LAAPPI-MSI. Red and blue colors indicate high and low abundancies, respectively. The heat map images show that betulinic acid is clearly more abundant in the lenticel regions of the analyzed sample areas (dashed boxes)

uniformly distributed in F1, and no clear distribution patterns were detected in addition to the compounds' lower abundances at the lenticel regions.

Conclusions

In this work, we applied ambient MS for the first time to the rapid analysis of plant metabolites directly from tree surface. DAPPI proved to be an efficient method for ionizing triterpenoids. Triterpenoids and other plant metabolites were detected from *B. pendula* bark fractions collected from three different developmental stages of the tree. The DAPPI-MS analysis showed unique chemical patterns for all the four studied bark fractions. The first two fractions of the mature stem (phellem and phelloderm tissues) were found to be rich with triterpenoids, but from the transition zone and the young apical stem, only the first fraction (phellem) of the bark was abundant with triterpenoids. The triterpenoids with the highest abundancies were betulin and lupeol. DAPPI-MS was also feasible for the screening of lenticels and the surrounding tissue from *B. pendula* and *A. glutinosa* F1 samples. The lenticels were shown to contain higher amounts of betulonic and betulinic acids than the surrounding tissue. The mature stem F1 of birch was also analyzed with LAAPPI-MSI, and the betulinic acid was detected with higher abundancy from the lenticels than from to the surrounding tissue. Thus it can be concluded that the LAAPPI-MSI measurements verified the DAPPI-MS results, and the sampling accuracy of DAPPI-MS was suitable for a proper analysis of lenticel-sized regions and the technique could be beneficial in rapid screening analysis of tree samples.

Acknowledgments Open access funding provided by University of Helsinki including Helsinki University Central Hospital. This study was supported by Academy of Finland projects #264621 and #275089. We thank GenoChem consortium for tree material, and Eija Rinne for excellent technical support.

Compliance with ethical standards

This article does not contain any studies with humans or animals performed by any of the authors.

Conflict of interest The authors declare that they have no conflict of interest.

References

1. Newman DJ, Cragg GM. Natural products as sources of new drugs from 1981 to 2014. J Nat Prod. 2016;79:629–61. https://doi.org/10.1021/acs.jnatprod.5b01055.
2. Alakurtti S, Mäkelä T, Koskimies S, Yli-Kauhaluoma J. Pharmacological properties of the ubiquitous natural product betulin. Eur J Pharm Sci. 2006;29:1–13. https://doi.org/10.1016/j.ejps.2006.04.006.
3. Fulda S. Betulinic acid for cancer treatment and prevention. Int J Mol Sci. 2008;9:1096–107. https://doi.org/10.3390/ijms9061096.
4. Krasutsky PA. Birch bark research and development. Nat Prod Rep. 2006;23:919–42. https://doi.org/10.1039/b606816b.
5. Haque S, Nawrot DA, Alakurtti S, Ghemtio L, Yli-Kauhaluoma J, Tammela P. Screening and characterisation of antimicrobial properties of semisynthetic betulin derivatives. PLoS One. 2014;9:e102696. https://doi.org/10.1371/journal.pone.0102696.
6. Saha S, Ghosh M, Dutta SK. A potent tumoricidal co-drug 'Bet-CA'—an ester derivative of betulinic acid and dichloroacetate selectively and synergistically kills cancer cells. Sci Rep. 2015;5:7762/1–7762/10. https://doi.org/10.1038/srep07762.
7. Li H, Webster D, Johnson JA, Gray CA. Anti-mycobacterial triterpenes from the Canadian medicinal plant Alnus incana. J Ethnopharmacol. 2015;165:148–51. https://doi.org/10.1016/j.jep.2015.02.042.
8. Ren X, He T, Chang Y, Zhao Y, Chen X, Bai S, et al. The genus *Alnus*, a comprehensive outline of its chemical constituents and biological activities. Molecules. 2017;22:1383/1–1383/37. https://doi.org/10.3390/molecules22081383.
9. Alonso-Serra J, Safronov O, Lim K, Fraser-Miller SJ, Blokhina OB, Campilho A, et al. Tissue-specific study across the stem reveals the chemistry and transcriptome dynamics of birch bark. New Phytol. 2019;222:1816–31. https://doi.org/10.1111/nph.15725.
10. Marston A, Hostettmann K. Natural product analysis over the last decades. Planta Med. 2009;75:672–82. https://doi.org/10.1055/s-0029-1185379.
11. Yrjönen T, Vuorela H, Kauppila TJ. Direct analysis of Peucedanum palustre samples by desorption atmospheric pressure photoionization-mass spectrometry. Phytochem Lett. 2017;20:49–53. https://doi.org/10.1016/j.phytol.2017.04.001.
12. Monge ME, Harris GA, Dwivedi P, Fernández FM. Mass spectrometry: recent advances in direct open air surface sampling/ionization. Chem Rev. 2013;113:2269–308. https://doi.org/10.1021/cr300309q.
13. Räsänen RM, Dwivedi P, Fernández FM, Kauppila TJ. Desorption atmospheric pressure photoionization and direct analysis in real time coupled with travelling wave ion mobility mass spectrometry. Rapid Commun Mass Spectrom. 2014;28:2325–36. https://doi.org/10.1002/rcm.7028.
14. Buchberger AR, DeLaney K, Johnson J, Li L. Mass spectrometry imaging: a review of emerging advancements and future insights. Anal Chem. 2018;90:240–65. https://doi.org/10.1021/acs.analchem.7b04733.
15. Bjarnholt N, Li B, D'Alvise J, Janfelt C. Mass spectrometry imaging of plant metabolites—principles and possibilities. Nat Prod Rep. 2014;31:818–37. https://doi.org/10.1039/C3NP70100J.
16. Haapala M, Pól J, Saarela V, Arvola V, Kotiaho T, Ketola RA, et al. Desorption atmospheric pressure photoionization. Anal Chem. 2007;79:7867–72. https://doi.org/10.1021/ac071152g.
17. Luosujärvi L, Arvola V, Haapala M, Pól J, Saarela V, Franssila S, et al. Desorption and ionization mechanisms in desorption atmospheric pressure photoionization. Anal Chem. 2008;80:7460–6. https://doi.org/10.1021/ac801186x.
18. Kauppila TJ, Arvola V, Haapala M, Pól J, Aalberg L, Saarela V, et al. Direct analysis of illicit drugs by desorption atmospheric

pressure photoionization. Rapid Commun Mass Spectrom. 2008;22:979–85. https://doi.org/10.1002/rcm.3461.
19. Kauppila TJ, Flink A, Haapala M, Laakkonen U, Aalberg L, Ketola RA, et al. Desorption atmospheric pressure photoionization-mass spectrometry in routine analysis of confiscated drugs. Forensic Sci Int. 2011;210:206–12. https://doi.org/10.1016/j.forsciint.2011.03.018.
20. Vaikkinen A, Schmidt HS, Kiiski I, Rämö S, Hakala K, Haapala M, et al. Analysis of neonicotinoids from plant material by desorption atmospheric pressure photoionization-mass spectrometry. Rapid Commun Mass Spectrom. 2015;29:424–30. https://doi.org/10.1002/rcm.7123.
21. Suni NM, Aalto H, Kauppila TJ, Kotiaho T, Kostiainen R. Analysis of lipids with desorption atmospheric pressure photoionization-mass spectrometry (DAPPI-MS) and desorption electrospray ionization-mass spectrometry (DESI-MS). J Mass Spectrom. 2012;47:611–9. https://doi.org/10.1002/jms.2992.
22. Vaikkinen A, Shrestha B, Kauppila TJ, Vertes A, Kostiainen R. Infrared laser ablation atmospheric pressure photoionization mass spectrometry. Anal Chem. 2012;84:1630–6. https://doi.org/10.1021/ac202905y.
23. Hieta JP, Vaikkinen A, Auno S, Räikkönen H, Haapala M, Scotti G, et al. A simple method for improving the spatial resolution in infrared laser ablation mass spectrometry imaging. J Am Soc Mass Spectrom. 2017;28:1060–5. https://doi.org/10.1007/s13361-016-1578-7.
24. Vaikkinen A, Shrestha B, Koivisto J, Kostiainen R, Vertes A, Kauppila TJ. Laser ablation atmospheric pressure photoionization mass spectrometry imaging of phytochemicals from sage leaves. Rapid Commun Mass Spectrom. 2014;28:2490–6. https://doi.org/10.1002/rcm.7043.
25. Yung YP, Wickramasinghe R, Vaikkinen A, Kauppila TJ, Veryovkin IV, Hanley L. Solid sampling with a diode laser for portable ambient mass spectrometry. Anal Chem. 2017;89:7297–301. https://doi.org/10.1021/acs.analchem.7b01745.
26. Härmä V, Haavikko R, Virtanen J, Ahonen I, Schukov H, Alakurtti S, et al. Optimization of invasion-specific effects of betulin derivatives on prostate cancer cells through lead development. PLoS One. 2015;10:e0126111/1–e0126111/22. https://doi.org/10.1371/journal.pone.0126111.
27. Haavikko R, Nasereddin A, Sacerdoti-Sierra N, Kopelyanskiy D, Alakurtti S, Tikka M, et al. Heterocycle-fused lupane triterpenoids inhibit Leishmania donovani amastigotes. MedChemComm. 2014;5:445–51. https://doi.org/10.1039/C3MD00282A.
28. Laavola M, Haavikko R, Hämäläinen M, Leppänen T, Nieminen R, Alakurtti S, et al. Betulin derivatives effectively suppress inflammation in vitro and in vivo. J Nat Prod. 2016;79:274–80. https://doi.org/10.1021/acs.jnatprod.5b00709.
29. Saarela V, Haapala M, Kostiainen R, Kotiaho T, Franssila S. Glass microfabricated nebulizer chip for mass spectrometry. Lab Chip. 2007;7:644–6. https://doi.org/10.1039/b700101k.
30. Kauppila TJ, Östman P, Marttila S, Ketola RA, Kotiaho T, Franssila S, et al. Atmospheric pressure photoionization-mass spectrometry with a microchip heated nebulizer. Anal Chem. 2004;76:6797–801. https://doi.org/10.1021/ac049058c.
31. McDonnell LA, Heeren RMA. Imaging mass spectrometry. Mass Spectrom Rev. 2007;26:606–43. https://doi.org/10.1002/mas.20124.
32. Kosyakov DS, Ul'yanovskii NV, Falev DI. Determination of triterpenoids from birch bark by liquid chromatography-tandem mass spectrometry. J Anal Chem. 2014;69:1264–9. https://doi.org/10.1134/S1061934814130061.
33. Rhourri-Frih B, Chaimbault P, Claude B, Lamy C, Andre P, Lafosse M. Analysis of pentacyclic triterpenes by LC-MS. A comparative study between APCI and APPI. J Mass Spectrom. 2009;44:71–80. https://doi.org/10.1002/jms.1472.
34. Sun Y, Feng F, Nie B, Cao J, Zhang F. High throughput identification of pentacyclic triterpenes in Hippophae rhamnoides using multiple neutral loss markers scanning combined with substructure recognition (MNLSR). Talanta. 2019;205:120011. https://doi.org/10.1016/j.talanta.2019.06.011.
35. Kauppila TJ, Kuuranne T, Meurer EC, Eberlin MN, Kotiaho T, Kostiainen R. Atmospheric pressure photoionization mass spectrometry. Ionization mechanism and the effect of solvent on the ionization of Naphthalenes. Anal Chem. 2002;74:5470–9. https://doi.org/10.1021/ac025659x.
36. Schymanski EL, Jeon J, Gulde R, Fenner K, Ruff M, Singer HP, et al. Identifying small molecules via high resolution mass spectrometry: communicating confidence. Environ Sci Technol. 2014;48:2097–8. https://doi.org/10.1021/es5002105.
37. Ferreira JPA, Quilhó T, Pereira H. Characterization of Betula pendula outer bark regarding Cork and Phloem components at chemical and structural levels in view of biorefinery integration. J Wood Chem Technol. 2017;37:10–25. https://doi.org/10.1080/02773813.2016.1224248.
38. Falev DI, Kosyakov DS, Ul'yanovskii NV, Ovchinnikov DV, Shestakov SL. Subcritical extraction of birch bark pentacyclic triterpenes. Russ Chem Bull. 2017;66:875–81. https://doi.org/10.1007/s11172-017-1822-8.
39. NIST Chemistry webbook. http://webbook.nist.gov/chemistry/. Accessed 8 Mar 2019
40. Laitinen J, Julkunen-Tiitto R, Rousi M, Heinonen J, Tahvanainen J. Ontogeny and environment as determinants of the secondary chemistry of three species of white birch. J Chem Ecol. 2005;31:2243–62. https://doi.org/10.1007/s10886-005-7100-5.
41. Liimatainen J, Karonen M, Sinkkonen J, Helander M, Salminen J. Characterization of phenolic compounds from inner bark of Betula pendula. Holzforschung. 2012;66:171–81. https://doi.org/10.1515/HF.2011.146.